AIP Journal of Applied Physics

A mathematical model of the modified Paschen's curve for breakdown in microscale gaps

David B. Go and Daniel A. Pohlman

Citation: Journal of Applied Physics **107**, 103303 (2010); doi: 10.1063/1.3380855
View online: http://dx.doi.org/10.1063/1.3380855
View Table of Contents: http://scitation.aip.org/content/aip/journal/jap/107/10?ver=pdfcov
Published by the AIP Publishing

A mathematical model of the modified Paschen's curve for breakdown in microscale gaps

David B. Go[1,a] and Daniel A. Pohlman[2]
[1]*Department of Aerospace and Mechanical Engineering, University of Notre Dame, Notre Dame, Indiana 46556, USA*
[2]*Department of Chemical and Biomolecular Engineering, University of Notre Dame, Notre Dame, Indiana 46556, USA*

(Received 28 September 2009; accepted 11 March 2010; published online 20 May 2010)

Traditionally, Paschen's curve has been used to describe the breakdown voltage for gaseous ionization between two electrodes. However, experiments have shown that Paschen's curve, which is based on Townsend effects, is not necessarily accurate in describing breakdown between electrodes spaced less than 15 μm apart. In this regime, electron field emission plays a significant role in the breakdown phenomenon, and recently an alternative mathematical description that accounts for ion-enhanced field emission was proposed to describe the breakdown voltage in small gaps. However, both Paschen's curve and the small gap equation only work in certain regimes, and neither predicts the transition that occurs between Townsend and field emission effects—the so-called modified Paschen's curve. In this work, a single, consistent mathematical description of the breakdown voltage is proposed that accounts for both Townsend ionization and ion-enhanced field emission mechanisms. Additionally, microscale breakdown experiments have been conducted in atmospheric air. The proposed formulation is compared to the present experiments and other atmospheric air experiments in the literature and describes the transition region in the breakdown curve. The proposed formulation represents a mathematical model for the modified Paschen's curve. © *2010 American Institute of Physics*. [doi:10.1063/1.3380855]

I. INTRODUCTION

Of main interest to this work is the initiation of plasma, when the discharge transitions from the non-self-sustaining to the self-sustaining regime. This transition occurs when an electron avalanche forms that leads to the breakdown of the gaseous dielectric medium (often called Townsend breakdown to distinguish it from space-charge induced streamer breakdown). Traditionally, Paschen's curve describes the breakdown voltage as a function of the electrode spacing or gap (d), operating pressure (p), and gas composition.[1] The mathematical formulation of Paschen's curve is derived from Townsend's description of the basic charge generation processes including electron impact ionization (the α process) and secondary electron emission from the cathode due primarily to ion bombardment (the γ process), though other bombardment processes may play a role.[2] Historically, Paschen's curve has proved to be accurate for large gaps and at low pressures,[3] but it is often acknowledged that it fails to describe behavior at extremely low or high pd values.[4] This has been especially true in very small gaps in atmospheric air.

In the 1950s, interest in atmospheric pressure, submillimeter discharges was fairly high, led by a series of papers out of Bell Laboratories[5–14] as well as others.[15] In the past decade or so, studies on atmospheric pressure, small gap discharges has undergone a resurgence, and the focus has turned to atmospheric air breakdown in microscale gaps on the scale of 1 to 30 μm. This recent interest was originally motivated by concerns about unintended breakdown leading to spark discharges and material erosion in microelectromechanical systems.[16–25] However, there have also been investigations of microscale breakdown in devices for gas sensing and analysis[26–30] and lighting applications[31] as part of the growth of the microplasma field. These works have led to a number of additional experimental,[32–35] computational,[36–39] and theoretical studies[40,41] to understand the nature of microscale breakdown.

Qualitatively, Paschen's curve predicts that the breakdown voltage decreases as the electrode gap decreases, corresponding with the increasing electric field. However, at some electrode gap the breakdown voltage reaches a minimum (approximately 300 V near 5 to 10 μm in atmospheric air), and the breakdown voltage then increases at successively smaller electrode gaps. This effect is because more energy is required in the system to overcome the rapid loss of electrons to surfaces in a microscale gap. However, many of these recent experimental studies have shown that as the electrode gap decreases below approximately 10 μm, the data deviate from Paschen's curve. Rather, the so-called *modified Paschen's curve*[20,23] is formed where the breakdown voltage continues to decrease nearly linearly with decreasing electrode gaps below the minimum predicted by Paschen's curve. Researchers from Bell Laboratories originally suggested that electron field emission will occur because of the high electric field in microscale gaps,[11,13,14] and these electrons will contribute to ionization and the overall current thereby mitigating the rapid charge loss. Slade and Taylor's[22] analysis showed that electron field emission in-

[a]Author to whom correspondence should be addressed. Electronic mail: dgo@nd.edu.

deed plays a critical role, and particle-in-cell Monte Carlo simulations by Zhang *et al.*[36] confirmed this hypothesis.

In 1955 Boyle and Kisliuk[11] proposed a theory for the effect of field emission on discharge current, where the emission is enhanced by positive ions approaching the cathode—henceforth called ion-enhanced field emission. Recently, Ramilović-Radjenović and Radjenović[40,41] used Boyle and Kisliuk's theory to formulate a new mathematical description of the breakdown voltage in microscale gaps due to ion-enhanced field emission. However, while Ramilović-Radjenović and Radjenović's breakdown voltage (henceforth called ion-enhanced field emission breakdown voltage) is accurate for microscale gaps it is not accurate for larger, mesoscale gaps where Paschen's curve still holds. Therefore, there are currently two separate, incompatible mathematical descriptions of the breakdown voltage, Paschen's curve for mesoscale gaps and ion-enhanced field emission for microscale gaps, and neither describes the transition between the two regimes. Further, a review of the experimental literature shows that there are anomalies in the transition behavior of discharges across these regimes, and the shape of the modified Paschen's curve is not consistent. To date, there is no mathematical model that consistently describes the modified Paschen's curve.

In this work, the authors present a mathematical formulation that combines Paschen's curve and ion-enhanced field emission to form the modified Paschen's curve. This work is focused on understanding the nature of the modified Paschen's curve in atmospheric air, and the proposed formulation is compared to experimental data from the literature and to present microscale breakdown experiments. Two distinct trends observed in experiments and simulations are highlighted, and the proposed formulation qualitatively describes both of these trends. While there are limitations to the proposed formulation, it appears to capture the transition from Paschen's curve to ion-enhanced field emission-dominated breakdown and accurately represents the modified Paschen's curve.

II. THEORETICAL APPROACH

A. Basic physical mechanisms

In the breakdown of a gas, usually termed Townsend's breakdown, there are two primary mechanisms that contribute to a significant rise in charge carriers—gaseous charge production through electron impact ionization (the α process) and cathode charge production through secondary emission (the γ process).[42] Secondary emission is electron emission due to bombarding particles/photons and is typically dominated by ions through Auger processes though incident photons and metastables can also be a factor. At sufficiently high electric fields ($\sim$100 V/μm), field emission may occur where electrons tunnel through the potential barrier at the cathode surface. With adequate geometric enhancement and a suitable material, emission at $\sim$10 V/μm is possible.[43] Recent detailed experiments by Hourdakis *et al.*[32] investigated the role of microsurface protrusions in microscale breakdown and showed that geometric surface enhancement is generally insufficient for the fields observed in breakdown experiments. Therefore, because geometric enhancement alone is insufficient, ion-enhanced field emission is likely the primary phenomenon that leads to microscale breakdown. Ion-enhanced field emission is like secondary emission but occurs when positive gaseous ions approach the cathode and both lower and thin the potential barrier at the cathode, thus making it easier for electrons to tunnel due to a high electric field. Kisliuk[14] investigated this mechanism and distinguished between a single ion approaching the cathode and the presence of many ions near the cathode, which is the more likely physical situation. In considering the effect of a single ion, he estimated that it would take an applied field of approximately 3000 V/μm for the ion-enhancement to yield a single field-emitted electron; but if reasonable geometric enhancement is included the applied field only needs to be 50 V/μm for ion-enhancement to initiate emission. A similar analysis was conducted by Ecker and Müller,[44] and more recent detailed analyses[45–48] have confirmed that ions can increase the emission current by one to three orders of magnitude. In the following analysis, only ion-induced secondary emission and ion-enhanced field emission are considered as the cathode processes in microscale breakdown.

B. Description of the processes

Townsend's first ionization coefficient α describes the generation of ions by electron impact and an empirical formula relates it to the applied voltage V, electrode gap g, and gas pressure p by

$$\alpha = Ape^{-Bpd/V}, \tag{1}$$

where A and B are constants based on the gas composition.[42] Secondary electron emission due to bombarding ions is characterized by Townsend's second ionization coefficient, which is defined as the ratio of electrons ejected per incident ion,

$$\gamma_i = n_{\text{secondary}}/n_{\text{ion}}. \tag{2}$$

In vacuum, the field emission current density from a metal is described by the Fowler–Nordheim equation[49]

$$j_{\text{field}} = \frac{A_{\text{FN}}\beta^2 E^2}{\phi t^2(y)} \exp\left[-\frac{B_{\text{FN}}\phi^{3/2} v(y)}{\beta E}\right], \tag{3}$$

where A_{FN} and B_{FN} are constants,[50] ϕ is the work function of the cathode, β is the geometric enhancement factor, and E is the magnitude of the applied electric field defined as $|E| = V/d$. The parameter y is a function of ϕ, β, and E, and the functions $t^2(y)$ and $v(y)$ have established approximations.[51] However, from empirical observations this relation can be written as

$$j_{\text{field}} = C_{\text{FN}} E^2 \exp\left[-\frac{D_{\text{FN}}}{E}\right], \tag{4}$$

where C_{FN} and D_{FN} are experimentally determined constants. Physically, D_{FN} is the threshold electric field required for field emission and is a function of the cathode material and surface properties[11]

$$D_{\text{FN}} = (6.85 \times 10^7)\frac{\phi^{3/2}}{\beta}\left[\frac{\text{V}}{\text{cm}}\right]. \tag{5}$$

C. Paschen's curve

Paschen's breakdown criterion is derived based on the increase in circuit current due to α and γ_i events. The prebreakdown current density takes the following form:

$$j_{\text{prebreakdown}} = \frac{j_o e^{\alpha d}}{1 - \gamma_i (e^{\alpha d} - 1)}, \tag{6}$$

where j_o is a background cathode emission current usually assumed to be photogenerated.[42] The breakdown criterion is then based on the mathematical condition where the current increases to infinity or

$$\gamma_i (e^{\alpha d} - 1) = 1. \tag{7}$$

Using this breakdown criterion, and the definition of α in Eq. (1), the breakdown voltage V_b is a function of the product of the gap and pressure pd and takes the following form:

$$V_b = \frac{Bpd}{\ln(pd) + \ln\left[\frac{A}{\ln(1/\gamma_i + 1)}\right]}. \tag{8}$$

Equation (8) produces the traditional Paschen's curve.

D. Ion-enhanced field emission breakdown voltage

In Boyle and Kisliuk's[11] theory for small gaps, breakdown is due to electron field emission that is enhanced by Townsend ionization in the gap—a positive feedback situation. Describing the emission current j_{field} based on the empirical Fowler–Nordheim equation, they suggest the local electric field is modified by some factor C_E by the approaching ion, enhancing the emission current by a factor C_j. The ion-enhanced field emission current, $j_{\text{field+}}$, is the prebreakdown current and is described by

$$j_{\text{field+}} = j_{\text{field}} e^{(M j_{\text{field+}}^n)}, \tag{9}$$

where n is a constant typically equal to unity and M is a constant that accounts for the enhancement factors C_E and C_j ($M = D_{\text{FN}} C_E C_j E^2$). Boyle and Kisliuk's breakdown criterion is based on the mathematic condition, where Eq. (9) is unstable. Because the emission of an electron is enhanced by an incident ion, they define an *effective* secondary emission coefficient γ' as the current of field-emitted electrons $j_{\text{field+}}$ per incident ion current j_{ion}, and derive it to be

$$\gamma' = \frac{j_{\text{field+}}}{j_{\text{field}}} = K e^{-D_{\text{FN}} d/V}, \tag{10}$$

where K is a constant that includes the constants in Eq. (4) and the enhancement constant C_E. It should be noted that in their original derivation, Boyle and Kisliuk used a form of the Fowler–Nordheim equation that did not have the E^2 prefactor shown in Eq. (4). In their derivation, K is actually a function of $1/E^2$ and they claim this dependence is small compared to the exponential term, thus ignoring it. However, if the Fowler–Nordheim equation shown in Eq. (4) is used, the E^2 and $1/E^2$ terms cancel thus resulting in a cleaner derivation of γ'.

Ramilović-Radjenović and Radjenović[40] defined the field emission breakdown voltage by treating γ' in Eq. (10) as the secondary emission coefficient in Eq. (7). They obtained the transcendental equation

$$K e^{-D_{\text{FN}} d/V_b} [e^{Apd \exp(-Bpd/V_b)} - 1] = 1. \tag{11}$$

This equation does not have a closed form solution for V_b and must be solved numerically. They simplified this equation by asserting that K is much larger than 1 ($\sim 10^7$) and the breakdown field occurs when V/d is greater than the threshold value D_{FN}. Therefore, taking logarithms of both sides and using a Taylor series expansion approximation (though this could also be done with a direct expansion of the exponential term), they rewrote the breakdown criterion as

$$\alpha d = \frac{1}{K} e^{-D_{FN} d/V_b}. \tag{12}$$

Using Eq. (1) for α, they showed that the breakdown voltage is given by[41]

$$V_b = \frac{d(D_{\text{FN}} + Bp)}{\ln(KApd)}. \tag{13}$$

The values of A and B are tabulated for many gasses, and D_{FN} is defined in Eq. (5), but K is not easily determined and essentially becomes a fitting parameter. It should be noted that in this formulation the breakdown voltage is no longer a function of pd but a function of p and d separately.

E. Modified Paschen's breakdown voltage—proposed mathematical description

The limitation of the ion-enhanced field emission breakdown voltage is that it uses an effective secondary emission coefficient γ' that is based *solely* on the effect of ion-enhanced field emission—an effect not present in larger gaps. A consistent description across electrode gaps, therefore, should potentially account for both ion-enhanced field emission and secondary emission due to ion bombardment. There are a number of bombardment mechanisms (ions, atoms, and metastables) that may contribute to secondary emission, and it has been shown before that if they are independent, their individual γ-factors may be summed.[42,52] Therefore it is assumed here that ion-induced secondary emission and ion-enhanced field emission are independent physical mechanisms. That is, the ejection of an electron due to an impacting ion (secondary emission) occurs independent of a field-emitted electron due to an approaching ion—and that a single ion may contribute to both. Mathematically, this can be expressed through superposition of the secondary emission current $j_{\text{secondary}}$ and enhanced field emission current $j_{\text{field+}}$ in the form of a net emission current,

$$j_{\text{emit}} = j_{\text{secondary}} + j_{\text{field+}}. \tag{14}$$

Using the same approach as Eq. (10) a net secondary emission coefficient can be defined as

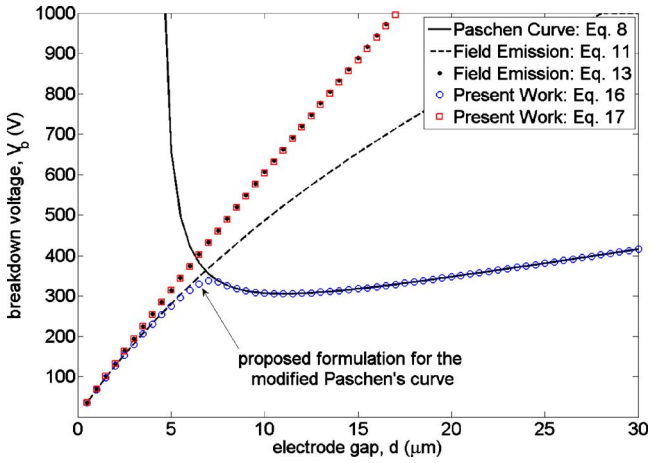

FIG. 1. (Color online) Paschen's breakdown voltage [Eq. (8)], the field emission breakdown voltages in transcendental form [Eq. (11)] and closed form approximation [Eq. (13)], and the proposed mathematical formulation [Eqs. (16) and (17)]. The constants for A and B are those for air (Ref. 42), $\beta=50$, $\phi=4.0$ eV, $\gamma=0.01$, and $K=10^7$.

$$\gamma_{\text{net}} = \frac{j_{\text{secondary}} + j_{\text{field+}}}{j_{\text{ion}}} = \gamma_i + \gamma'. \tag{15}$$

In a manner similar to that used by Ramilović-Radjenović and Radjenović, γ_{net} can be inserted into the breakdown criterion Eq. (7) to give the following equation:

$$(\gamma_i + Ke^{-D_{FN}d/V})[e^{Apd\exp(-Bpd/V)} - 1] = 1. \tag{16}$$

This equation can also be simplified using a Taylor expansion to be

$$\gamma_i Apde^{-Bpd/V_b} + KApde^{-(Bpd+D_{FN}d)/V_b} = 1. \tag{17}$$

Note that neither the general breakdown voltage equation Eq. (16), nor the simplified form Eq. (17), have closed form solutions for V_b.

III. THEORETICAL RESULTS

As qualitatively described by Wallash and Levit,[23] the modified Paschen's curve roughly consists of three regions: the "pure" Paschen curve at gaps greater than 10 μm, a plateau between 5 to 10 μm, and a steep decline associated with field emission for gaps less than 5 μm. Dhariwal *et al.*,[18] in slight contrast, suggested there are actually four regions—splitting the field emission domain into an ion-enhanced region (1.5 to 5 μm) and a pure Fowler–Nordheim field emission (for metals) region in very small gaps ($<$1.5 μm). The defining characteristic of both descriptions is a plateau region that transitions from Townsend dominated processes to a field emission-dominated process, and consists of a flattening of the breakdown curve near the minimum voltage predicted by Paschen's curve.

Figure 1 shows a plot of Paschen's curve [Eq. (8)], the solutions to the transcendental ion-enhanced field emission equation [Eq. (11)] and in Taylor-expanded closed form [Eq. (13)], and the modified Paschen's curve proposed here in full form [Eq. (16)] and Taylor-expanded [Eq. (17)]. It is evident that the proposed mathematical relation Eq. (16) transitions from large gaps to small gaps in a continuous manner—effectively unifying Paschen's curve with ion-enhanced field emission. To that end, Eq. (16) inherently describes how Townsend processes dominate field emission at larger, mesoscale gaps, in the transition region both effects are present as seen in the characteristic plateau, and in microscale gaps ion-enhanced field emission dominates. It is also apparent that Eq. (17) fails to consistently describe the data during the transition to large gaps, and this can readily be attributed to the Taylor expansion approximation, which is only valid for small values of d. In fact, it can be shown that using the Taylor expansion approximation in the derivation of Paschen's curve leads to a nonphysical condition where V_b is always less than zero. Though this plot extends below 3 μm, the validity of these equations in this regime is questionable. The mean free path of an electron in air is $\sim$400 nm and the ionization mean free path is $\sim$1 μm, which means there is insufficient space to generate an appreciable number of ions. Therefore, at these scales the current is due only to pure field emission, and these equations, which are dependant on the existence of ions, are essentially invalid as will be discussed in Sec. V. Ultimately, Eq. (16) is the proposed formulation for the modified Paschen's curve.

IV. EXPERIMENTS

A number of experimental microscale breakdown studies using various electrode materials, geometries, gases, and gas pressures have been conducted preceding this work, and these are summarized in Table I (though this is not an exhaustive list). In most cases, the electrode materials are common microfabrication materials such as silicon (Si), platinum (Pt), and gold (Au), though other materials have also been studied. There are two general experimental configurations—the two electrodes are maintained at a small gap by an external micropositioning system or two planar electrodes are microfabricated on the surface of a substrate. The primary gas of interest is air at atmospheric pressure, though other common gases such as argon (Ar) and nitrogen (N_2) have also been studied, and pressures have ranged from 0.3 to 7500 torr.

To complement the existing experimental data and highlight some of the significant trends, a set of simplified experiments was conducted here. Two different anodes, a hollow copper (Cu) cylinder with 880 μm inner diameter and 1600 μm outer diameter and a stainless steel (SS) needle with a tip curvature of approximately 20 μm as verified by scanning electron microscopy, and a single cathode consisting of a large copper plate were tested. The electrodes were operated in a point-to-plane configuration (Fig. 2), and the gap was varied from 3 to 20 μm and maintained by fixing the cathode and adjusting the position of the anode using a Newport MFA-CC motorized linear stage micropositioning system with an accuracy of 0.1 μm. Positive electric potential was applied to the anode using a Bertran 228–10R high voltage power supply that had uncertainty of approximately 1 V, and the cathode was grounded. The current was recorded at the grounded cathode using a Keithley 6487 picoammeter. The electric potential was increased an increment of 5 V, allowed 5 s to settle, and then 20 current

TABLE I. Representative recent experimental studies of microscale breakdown phenomena. Standard material abbreviations have been employed. Planar refers to planar devices microfabricated onto a substrate.

Year	Author	Materials (c)=cathode and (a)=anode	Configurations	Gases	Pressures (torr)	Gaps (μm)
1999	Torres and Dhariwal (Refs. 16 and 17)	Cu, Fe, Al, Ni, brass	sphere-to-plane, cylinder-to-plane	air	0.3–760	0.5–25
2000	Dhariwal *et al.* (Ref. 18)	Cu, Fe, Al, Ni, brass	cylinder-to-plane	air, N_2	760–3040	0.5–15
2000	Ono *et al.* (Ref. 19)	Si, Si with Au coating, Pt	planar	air	760	0.6–7
2001	Lee *et al.* (Ref. 20)	Fe (c), Ag (a)	point-to-plane	air	760	0.1–40
2001	Ito *et al.* (Ref. 21)	Pt, W, Au	planar	air, Ar, He, H_2, CH_4-H_2	75–7500	1–40
2003	Wallash and Levit (Ref. 23)	Cr	planar	air	760	0.9–4
2003	Longwitz *et al.* (Ref. 26)	Pt, Au	planar	air, Ar, N_2	$7.5\times10^{-6}-1275$	1–50
2006	Hsieh and Jou (Ref. 34)	Ti, TiN	planar	Ar	1–760	20
2006	Chen *et al.* (Ref. 24)	n-type Si, p-type Si, Al	planar	air	760	2–21
2006	Hourdakis *et al.* (Refs. 32 and 33)	Au	plane-to-plane	air	760	0.4–45
2008	Strong *et al.* (Ref. 25)	Si	planar	air	760	2–7
2008	Sismangolu and Amorim (Ref. 35)	Cu	hollow cathode	air	760	5–20
2009	Go *et al.* (Ref. 29)	Ti, Al	planar	air	760	5–20
Present work	Go and Pohlman	Cu (c), Cu (a), SS (a)	point-to-plane	air	760	3–20

readings were averaged. This process was repeated until breakdown was observed when the current rapidly increased from less than 1 nA to hundreds or thousands of μA. At the occurrence of breakdown, the voltage was quickly reduced to zero. The experiments were conducted in open, atmospheric air, which, though not ideal, is not uncommon because it represents real operating conditions for many devices.[19,20,25,28,29,32,33] Additionally, because the purpose of these experiments was simply to show trends, control or analysis of the electrodes' surface quality was not conducted, though they were cleaned in acetone before every test to limit contamination effects. For experiments with detailed surface analysis, the reader is directed elsewhere (e.g., Ref. 32).

Figure 3 collects data from results reported by others and the present experiments in the form of breakdown curves for atmospheric air. Because of the plethora of data, individual sets are not distinguished here, save for the present work, but Table II details the sources of data included in the figure. It is readily apparent that in most of the cases, including the present experiments, the data deviate from the theoretical Paschen's curve in gaps less than 10 μm to form the modified Paschen's curve. This qualitatively confirms the form of the curve predicted by Eq. (16) in Fig. 1. In larger, mesoscale gaps, the data generally have the same shape and slope as Paschen's curve but the range of voltages is large, with data for any given electrode gap varying by as much as 200 V.

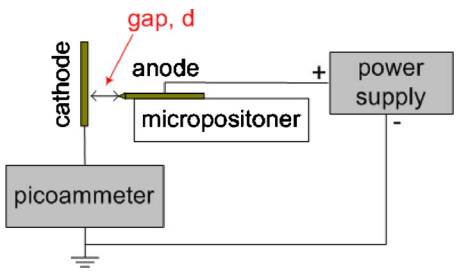

FIG. 2. (Color online) Schematic of the experimental apparatus in open, atmospheric air using a copper plate cathode and SS needle or Cu hollow cylinder anode.

This is not unexpected given that Paschen's curve is defined for a uniform electric field—a condition that is not always true in the various experimental studies. This effect is highlighted by the two curves representing the present experiments with the SS needle tip anode and Cu hollow cylinder anode. Though the Cu plate cathode, which supplies electrons through secondary and/or field emission, is the same in both cases, the breakdown curves are qualitatively quite different. The SS curve follows a fairly constant decreasing trend between the breakdown voltage and electrode gap—consistent with much of the other data. The hollow Cu cylinder curve, though, appears to follow Paschen's curve by reaching a local voltage minimum and increasing before sharply deviating from Paschen's curve as the gap continues to decrease. Overall, Fig. 3 highlights the complexity of breakdown at the microscale, where general trends are common but quantitative data are heavily dependant on the electrode geometry, material, and surface roughness.

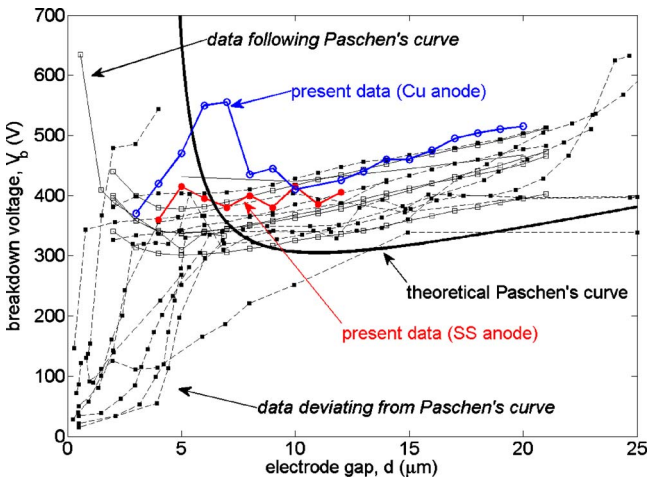

FIG. 3. (Color online) Breakdown voltage vs electrode gap in atmospheric air for a number of studies in the literature (see Table II), the present data, and the theoretical Paschen's curve. Studies from the literature with symbol ■ deviate from Paschen's curve and those with symbol □ qualitatively follow Paschen's curve. Note: line segments connecting data points are not curve fits but meant to clearly show the data shape and trends.

TABLE II. Summary of experimental data presented in Fig. 2. The data are extracted from figures in the original publications, and these are included in the third column.

Year	Author	Figure in original publication	Comments
1999	Torres and Dhariwal (Ref. 17)	Figure 4	data for Al, Ni, and brass
2000	Dhariwal *et al.* (Ref. 18	Figure 9	Ni
2000	Ono *et al.* (Ref. 19)	Figure 15	data for Si and Pt
2001	Lee *et al.* (Ref. 20)	Figure 6	data for only a 500 V offset voltage
2002	Slade and Taylor (Ref. 22)	Figure 2	presented data extrapolated from Lee *et al.* (Ref. 20)
2003	Wallash and Levit (Ref. 23)	Figure 8	
2006	Chen *et al.* (Ref. 24)	Figures 5–7	data for n-type Si, p-type Si, and Al—both planar and comb configurations
2006	Hourdakis *et al.* (Ref. 32)	Figure 6	
2009	Go *et al.* (Ref. 29)	Figure 10	data for Ti on Si substrate

In particular, three different behaviors are highlighted in Fig. 4, which shows a subset of data in Fig. 3. The first is the modified Paschen's curve with a plateau [Fig. 4(a)] that represents most of the data in Fig. 3. The second is a form of the modified Paschen's curve where, rather than going through a smooth, plateau transition from Townsend to field emission, Paschen's curve is sustained in decreasingly smaller gaps until field emission quickly initiates and dominates the discharge [Fig. 4(b)]. Therefore, rather than a plateau, this modified Paschen's curve has a local minimum voltage and is followed by a sharp transition. This case includes the data compiled by Slade and Taylor,[22] the present hollow Cu cylinder work, and simulation results of Zhang *et al.*[36] (Note: the data from Slade and Taylor was extracted from the results of Lee *et al.*,[20] who conducted experiments at a variety of supply voltages. Slade and Taylor did not specify which data points of Lee *et al.*'s they choose, and because of the density of points and limited quality of the image, it is difficult to extract identical points from Lee *et al.*'s original publication. However, Slade and Taylor's work is an oft-cited, well-respected work on this topic, and the data points they presented are presumed valid.) In Sec. V, Eq. (16) is curve fit to the data shown in Figs. 4(a) and 4(b)

Not all reported experiments showed the "modified" form and, in particular, Si electrodes[19,24] appeared to follow Paschen' s curve even at very small gaps [Fig. 4(c)]. Si is a semiconductor, and semiconductor field emission is different than that from metals.[53] Therefore, the fact that Si electrodes follow the traditional Paschen's curve could indicate a delay in field emission associated with their semiconducting properties.

V. COMPARISON TO EXPERIMENTS

Equation (16) was curve fit to the data for the modified Paschen's curves in Figs. 4(a) and 4(b), and these are shown in Figs. 5 and 6, respectively. The values of the work function were assumed to be that of the bulk materials in each experiment,[54] and the parameters β and K were varied until the fit was reasonably good. Typical values for β were approximately 50 to 100, reasonable values for most materials, and K was on the order of 10^8 to 10^9, which are little high but not that much higher than the values ($\sim 10^7$) extracted from Refs. 11 and 41. However, in each case, this single mathematical relation is able to qualitatively recreate the observed experimental and computational trends and shapes. In particular, Eq. (16) predicts both shapes of the modified Paschen curve. In Fig. 5, Eq. (16) accurately predicts the "plateau" transition from Fig. 4(a), and shows a smooth transition from Townsend to ion-enhanced field emission dominated breakdown. If the value of K is decreased as shown in Fig. 6, Eq. (16) predicts the sharp transition in Fig. 4(b) from Townsend to field emission breakdown, including a local minimum voltage. Further, Figs. 5 and 6 are representative of curve fits to other data sets presented in Fig. 2 indicating the proposed formulation is fairly robust. Though matching the experimental data is not conclusive evidence that Eq. (16) is correct, the fact that the single equation accurately captures all trends lends confidence to the validity of the formulation.

The role of the fitting parameter K is further explored in Fig. 7(a), where breakdown voltages are plotted for different values of K. Recall that the physical meaning of K is closely tied to the local enhancement of the electric field by an approaching ion (C_E) as well as other field emission parameters including β and ϕ. To that end, smaller K values correlate to a smaller ion-enhanced field emission effect, and larger K values correlate to a larger ion-enhanced field emission effect. As observed in Fig. 7(a), for a larger value of K the plateau form of modified Paschen's curve is recovered, and as K decreases, the sharp transition form is captured. The local peak in the breakdown voltage at transition, shown in Fig. 7(a), was determined for each curve, and the electric field at this transition point was calculated. The electric field ranged from 150 $\mathrm{V}/\mu\mathrm{m}$ for small K to 30 $\mathrm{V}/\mu\mathrm{m}$ for large K—reasonable fields for ion-enhanced field emission to initiate[14] and start competing with secondary emission. The effect of β and ϕ were also explored for a fixed constant K. A similar trend as shown in Fig. 7(a) was also observed, though not presented here for brevity. Generally, as β increased or ϕ decreased, the modified Paschen curve shape transformed from the sharp transition to the plateau form. Further, it was observed that the small changes in β had a much greater effect than small changes in ϕ. However, it is worth noting that changes in β and ϕ *inherently imply changes in* K, and it is not realistic to hold K constant. That is, while it is notable that β appears to have a greater impact than ϕ, further study is required to fully understand this relationship. The mutual contribution by both processes across most electrode gaps is also apparent in the shape of the modified Paschen curve in Fig. 7(a). Though the curve *appears* to be linear as it trends toward zero, it is not linear.

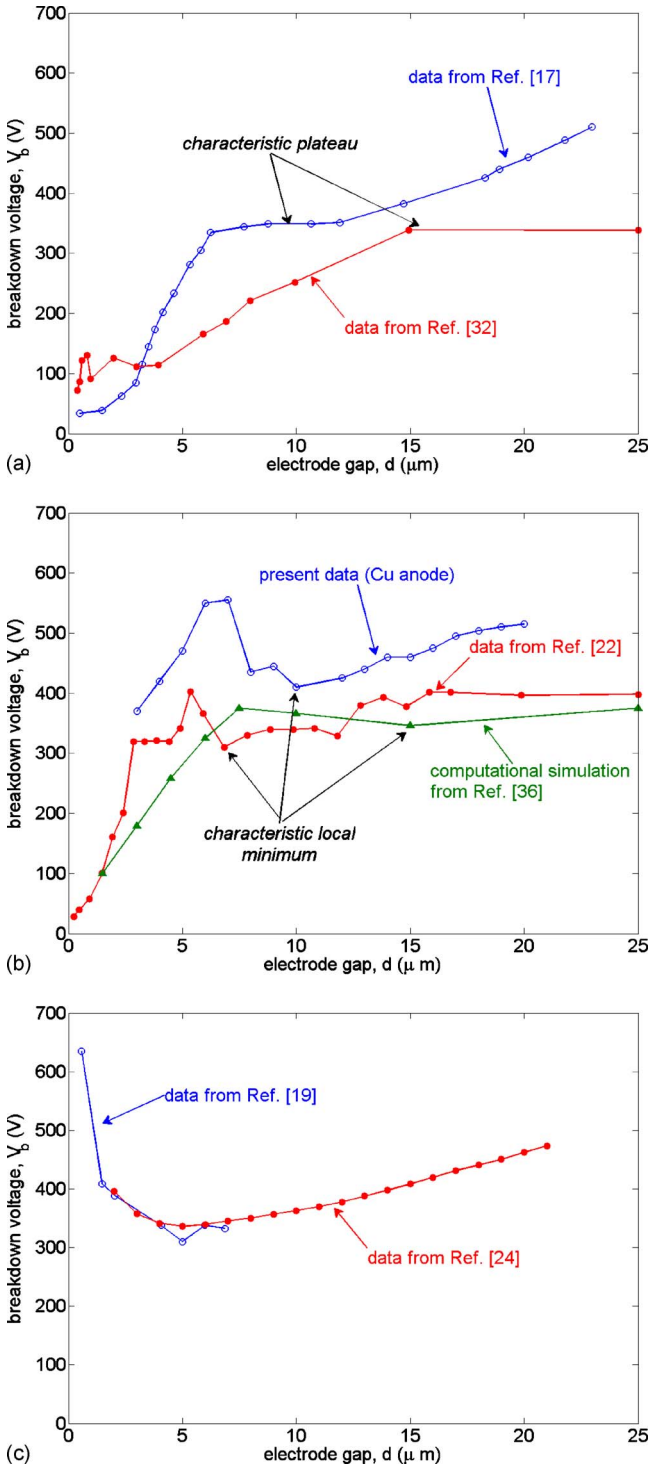

FIG. 4. (Color online) Select data to show three distinct breakdown behaviors in atmospheric air: (a) modified Paschen curve with plateaus including data from Refs. 17 and 32, (b) modified Paschen curves without plateaus including present data, data from Ref. 22, and computational simulations (Ref. 36), and (c) pure Paschen's curves including data from Refs. 19 and 24. Note: line segments connecting data points are not curve fits but meant to clearly show the data shape and trends.

Whereas a linear curve would apply for pure field emission,[23] the nonlinearity is due to the inclusion of Townsend processes—consistent with Dhariwal *et al.*'s description of four breakdown regions.[18]

In Fig. 7(b), the ratio of the ion-enhanced field emission secondary coefficient γ' [Eq. (10)] to Townsend's secondary

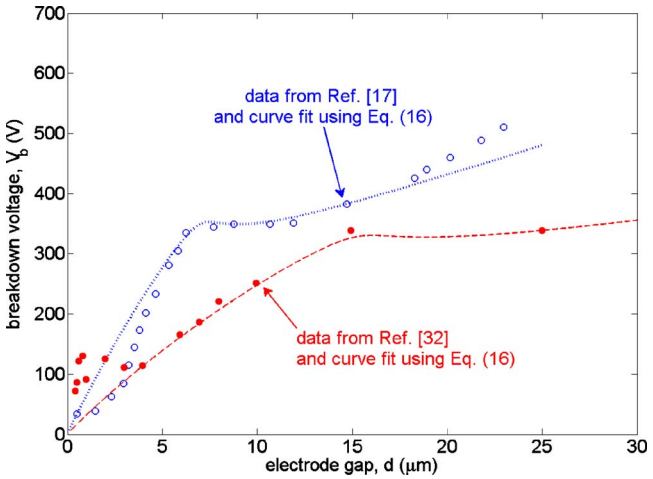

FIG. 5. (Color online) Breakdown curves in atmospheric air from Refs. 17 and 32 and curve fits using Eq. (16).

coefficient γ (held constant at 0.01) is plotted against the electrode gap for the same values of K. The ratio γ'/γ spans many orders of magnitude as the breakdown transitions from Townsend dominated to field emission-dominated processes. Of particular note, is that at larger, mesoscale gaps when Paschen's curve holds true (>15 μm), the ratio is extremely small ($<10^{-8}$) suggesting that ion-enhanced field emission is negligible. However, in moderately small microscale gaps from approximately 3 μm until the peak voltage transition, the ratio is moderate ($\sim 10^{-2}$ to 10^{1}) indicating that though field emission is now important, Townsend secondary emission cannot be ignored. To that end, the value of the ratio γ'/γ was also calculated at the transition point corresponding to the local peak in the breakdown voltage. Though not a constant as might have been expected, the ratio consistently was on the order of 10^{-2} to 10^{-1}, and always less than 1. This suggests that breakdown begins deviating from Paschen's curve when only 1%–10% of the emitted electrons are generated by ion-enhanced field emission rather than secondary emission. In very small microscale gaps (<3 μm) the ratio becomes large ($\sim 10^{2}$) and given that γ was fixed at 0.01,

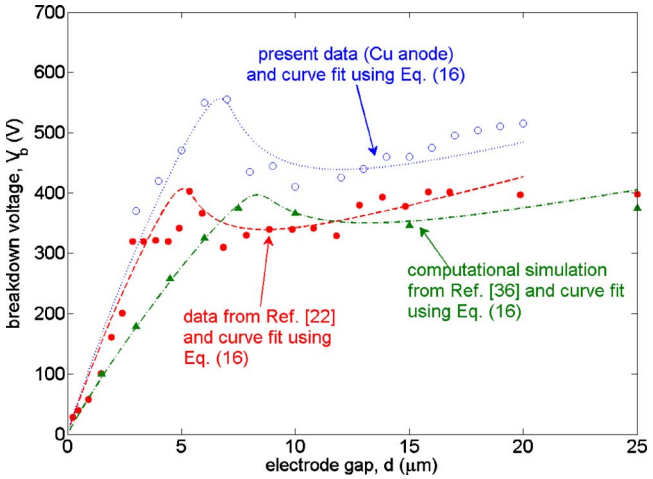

FIG. 6. (Color online) Breakdown curves in atmospheric air from the present data, Ref. 22, and computational simulations (Ref. 36) and curve fits from Eq. (16).

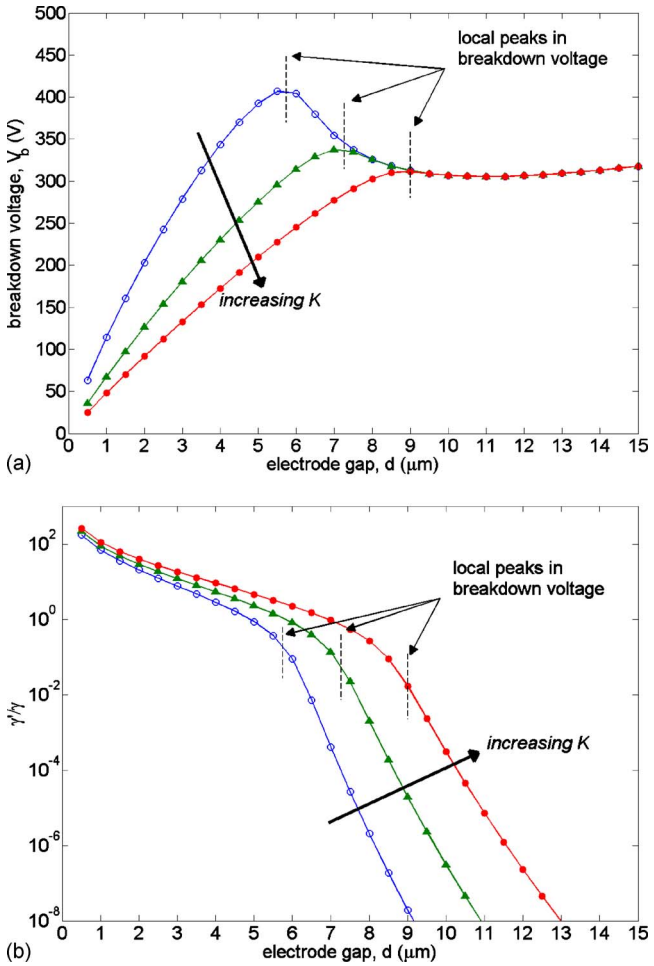

FIG. 7. (Color online) (a) Plot of modified Paschen's curves [Eq. (16)] and (b) the ratio of γ'/γ for different values of K. The constants for A and B are those of air (Ref. 42) β=50, ϕ=4.0 eV, and γ=0.01. The vertical dashed lines indicate the local peak in the breakdown voltage at the transition to field emission.

this corresponds to $\gamma' \approx 1$. A secondary emission coefficient of 1 is typically nonphysical except in special cases, and this merely confirms that this description of breakdown is not appropriate at very small gaps.

VI. CONCLUSIONS

In this work, a mathematical expression has been presented that consistently describes the breakdown voltage in microscale gaps when breakdown deviates from Paschen's curve. This formulation for the modified Paschen's curve is based on the assumed independence of two cathode emission effects—secondary emission due to ion bombardment and ion-enhanced field emission. Comparison with both experimental and simulation results show that this formulation for modified Paschen's curve captures the nature of the transition from Paschen's curve to field emission-dominated breakdown. Coupled with others' prior studies, the present results add further confidence that ion-enhanced field emission initiates in the transition region even at gaps as large as 10 μm. Future experimental and theoretical studies will explore the form and validity of the modified Paschen's curve in other pressure regimes—both greater than and less than atmospheric pressure—and other gases.

Two weaknesses of this formulation are that it accounts for ion-enhanced field emission through a fitting parameter and its inability to describe pure field emission in gaps less than approximately 2 μm. To that end, future work on this topic should focus on establishing a breakdown theorem that (a) has well-defined *ab initio* parameters for ion-enhanced field emission and (b) accounts for both ion-enhanced and standard Fowler–Nordheim field emission to completely describe all four regions of microscale breakdown. Thus, while this derivation represents an important step in understanding breakdown phenomenon in small gaps, it is not necessarily a definitive equation, and more eloquent derivations may be possible.

ACKNOWLEDGMENTS

The authors wish to thank Dr. Davide Mariotti for reviewing the manuscript and offering helpful feedback. D.A.P. wishes to acknowledge funding through a University of Notre Dame Center for Nano Science and Technology Nanoelectronics Undergraduate Research Fellowship.

[1]F. Paschen, Ann. Phys. **273**, 69 (1889).
[2]J. Townsend, *Electricity in Gases* (Oxford University Press, Oxford, 1915).
[3]T. W. Dakin, G. Luxa, G. Oppermann, J. Vigreux, G. Wind, and H. Winkelnkemper, Electra **32**, 61 (1974).
[4]E. Nasser, *Fundamentals of Gaesous Ionization and Plasma Electronics* (Wiley, New York, 1971).
[5]L. H. Germer, J. Appl. Phys. **22**, 955 (1951).
[6]L. H. Germer, J. Appl. Phys. **22**, 1133 (1951).
[7]L. H. Germer and J. L. Smith, J. Appl. Phys. **23**, 553 (1952).
[8]L. H. Germer, J. Appl. Phys. **25**, 332 (1954).
[9]P. Kisliuk, J. Appl. Phys. **25**, 897 (1954).
[10]W. S. Boyle and L. H. Germer, J. Appl. Phys. **26**, 571 (1955).
[11]W. S. Boyle and P. Kisliuk, Phys. Rev. **97**, 255 (1955).
[12]L. H. Germer and J. L. Smith, Bell Syst. Tech. J. **36**, 769 (1957).
[13]L. H. Germer, J. Appl. Phys. **30**, 46 (1959).
[14]P. Kisliuk, J. Appl. Phys. **30**, 51 (1959).
[15]R. M. Schaffert, IBM J. Res. Dev. **6**, 192 (1962).
[16]J.-M. Torres and R. S. Dhariwal, Microsyst. Technol. **6**, 6 (1999).
[17]J.-M. Torres and R. S. Dhariwal, Nanotechnology **10**, 102 (1999).
[18]R. S. Dhariwal, J.-M. Torres, and M. P. Y. Desmulliez, IEE Proc.: Sci., Meas. Technol. **147**, 261 (2000).
[19]T. Ono, D. Y. Sim, and M. Esashi, J. Micromech. Microeng. **10**, 445 (2000).
[20]R.-T. Lee, H.-H. Chung, and Y.-C. Chiou, IEE Proc.: Sci., Meas. Technol. **148**, 8 (2001).
[21]T. Ito, T. Izaki, and K. Terashima, Thin Solid Films **386**, 300 (2001).
[22]P. G. Slade and E. D. Taylor, IEEE Trans. Compon. Packag. Tech. **25**, 390 (2002).
[23]A. Wallash and L. Levit, Proc. SPIE **4980**, 87 (2003).
[24]C.-H. Chen, J. A. Yeh, and P.-J. Wang, J. Micromech. Microeng. **16**, 1366 (2006).
[25]F. W. Strong, J. L. Skinner, and N. C. Tien, J. Micromech. Microeng. **18**, 075025 (2008).
[26]R. G. Longwitz, H. van Lintel, and P. Renaud, J. Vac. Sci. Technol. B **21**, 1570 (2003).
[27]D. Mariotti, J. A. McLaughlin, and P. Maguire, Plasma Sources Sci. Technol. **13**, 207 (2004).
[28]M. S. Peterson, W. Zhang, T. S. Fisher, and S. V. Garimella, Plasma Sources Sci. Technol. **14**, 654 (2005).
[29]D. B. Go, T. S. Fisher, S. V. Garimella, and V. Bahadur, Plasma Sources Sci. Technol. **18**, 035004 (2009).
[30]J. Huang, J. Wang, C. Gu, K. Yu, F. Meng, and J. Liu, Sens. Actuators, A **150**, 218 (2009).

[31]Z. L. Petrović, N. Škoro, D. Marić, C. M. O. Mahony, P. D. Maguire, M. Radmilović-Rađenović, and G. Malović, J. Phys. D **41**, 194002 (2008).
[32]E. Hourdakis, G. W. Bryant, and N. M. Zimmerman, J. Appl. Phys. **100**, 123306 (2006).
[33]E. Hourdakis, B. J. Simonds, and N. M. Zimmerman, Rev. Sci. Instrum. **77**, 034702 (2006).
[34]C.-F. Hsieh and S. Jou, Microelectron. J. **37**, 867 (2006).
[35]B. N. Sismangolu and J. Amorim, Eur. Phys. J. Appl. Phys. **41**, 1465 (2008).
[36]W. Zhang, T. S. Fisher, and S. V. Garimella, J. Appl. Phys. **96**, 6066 (2004).
[37]M. Radmilović-Radjenović, J. K. Lee, F. Iza, and G. Y. Park, J. Phys. D **38**, 950 (2005).
[38]M. Radmilović-Radjenović and B. Radjenović, IEEE Trans. Plasma Sci. **35**, 1223 (2007).
[39]M. Radmilović-Radjenović and B. Radjenović, Plasma Sources Sci. Technol. **16**, 337 (2007).
[40]M. Radmilović-Radjenović and B. Radjenović, Plasma Sources Sci. Technol. **17**, 024005 (2008).
[41]M. Radmilović-Radjenović and B. Radjenović, EPL **83**, 25001 (2008).
[42]Y. P. Raizer, *Gas Discharge Physics* (Springer, New York, 1991).
[43]D. G. Walker, C. T. Harris, T. S. Fisher, and J. L. Davidson, Diamond Relat. Mater. **14**, 113 (2005).
[44]G. Ecker and K. G. Müller, J. Appl. Phys. **30**, 1466 (1959).
[45]P. Testé and J.-P. Chabrerie, J. Phys. D **29**, 697 (1996).
[46]R. Gayet, C. Harel, T. Josso, and H. Jouin, J. Phys. D **29**, 3063 (1996).
[47]C. Spataru, D. Teillet-Billy, J. P. Gauyacq, P. Testé, and J.-P. Chabrerie, J. Phys. D **30**, 1135 (1997).
[48]T. Josso, H. Jouin, C. Harel, and R. Gayet, J. Phys. D **31**, 996 (1998).
[49]R. Fowler and L. Nordheim, Proc. R. Soc. London, Ser. A **119**, 173 (1928).
[50]R. Good and E. Müller, in *Field Emission, Encyclopedia of Physics*, edited by S. Flugge (Springer-Verlag, Berlin, 1957), Vol. 21, pp. 176–231.
[51]C. Spindt, I. Brodie, L. Humphrey, and E. Westerberg, J. Appl. Phys. **47**, 5248 (1976).
[52]A. V. Phelps and Z. Lj. Petrovic, Plasma Sources Sci. Technol. **8**, R21 (1999).
[53]R. Stratton, Phys. Rev. **125**, 67 (1962).
[54]CRC, *Handbook of Chemistry and Physics*, 68th ed., edited by R. Weast (CRC, Cleveland, 1987).